arXiv:nucl-ex/0404019v1 14 Apr 2004

High-p_T electron distributions in d+Au and p+p collisions at RHIC

A. A. P. Suaide for the STAR Collaboration‡

Instituto de Física, Universidade de São Paulo
Po. Box 66318, 05315-970, São Paulo, SP, Brazil

Abstract. We present preliminary measurements of electron and positron spectra in d+Au and p+p collisions at $\sqrt{s_{NN}} = 200$ GeV for $1.5 < p_T < 7.0$ GeV/c. These measurements were carried out using the STAR Time Projection Chamber (TPC) and the Barrel Electromagnetic calorimeter (EMC). Overall hadron rejection factors in the range of 10^5 have been achieved. In this work we describe the measurement technique used to discriminate electrons from hadrons and compare the results for single electron spectra with Pythia based pQCD calculations for electrons from heavy-quark semi-leptonic decays.

The primary electron spectrum over a sufficiently broad p_T range provides a measurement of charm and beauty production at RHIC energies. In heavy ion collisions, these heavy quark production rates are expected to be an important diagnostic of the dense system formed in the collision. In particular, comparative measurements in p+p, d+Au and Au+Au will provide important sensitivity to the initial state gluon densities in these systems [1] and medium effects such as heavy quark energy loss. The suppression of small angle gluon radiation for heavy quarks would decrease the amount of energy loss (dead cone effect) [2] and, if gluon bremsstrahlung is indeed the main mechanism of quark energy loss, the suppression of heavy quark mesons at high-p_T is expected to be smaller than that one observed for charged hadrons at RHIC [3]. This comparison is an important check of the quenching mechanism at heavy-ion collisions. Moreover, measuring open charm and beauty production at RHIC provides essential reference data for studies of color screening via quarkonium suppression [4].

The results presented in this work were obtained with the STAR detector using the Time Projection Chamber (TPC) and the first EMC patch installed for the 2003 RHIC run, which consisted of 60 modules, half of the full planned detector, with coverage from $0 < \eta < 1$ and $\Delta\phi = 360^o$. Each one of the EMC modules is divided into 40 towers with spatial coverage of $(\Delta\eta, \Delta\phi) = (0.05, 0.05)$. The tower depth is 21 radiation lengths (X_0). A Shower Max Detector (SMD) is located approximately 5 X_0 deep inside the calorimeter module and allows to measure the electromagnetic shower shape and position with high precisison $(\Delta\eta, \Delta\phi) \sim (0.007, 0.007)$. Details about the detectors used in this analysis can be found in Ref. [5].

‡ For the full author list and acknowledgements see Appendix "Collaborations" in this volume.

The process of electron identification using the STAR barrel calorimeter is based on a pre-selection of electron candidates from the TPC dE/dx measurement. Electrons in the momentum range between 1.5 and 8 GeV/c have slightly higher dE/dx values when compared to hadrons. A dE/dx cut in this momentum range provides initial discimination power on the order of $e/h \sim 500$ with high efficiency.

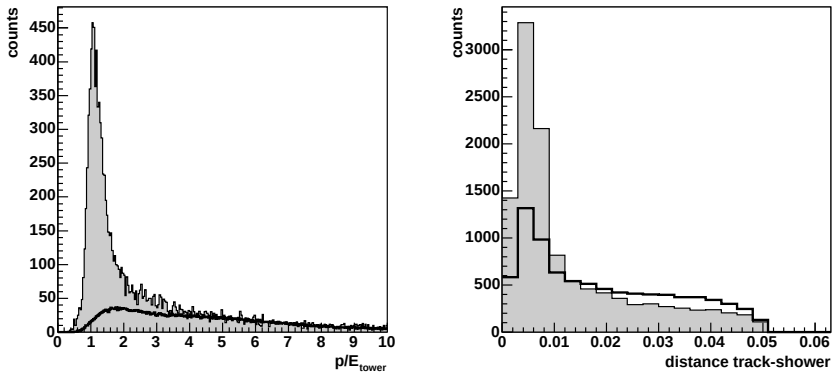

Figure 1. Left: p/E_{tower} distributions. Right: Distance between extrapolated track and Shower Max detector shower position. Shadowed histograms are the distributions for electrons and the non-shadowed ones are distributions for hadrons.

After the electron candidates are selected, they are extrapolated to the EMC detector and the energy deposited in the tower hit by the candidate is compared to its momentum. Electrons should show a peak at $p/E_{tower} \sim 1$. Hadrons have a wider distribution of p/E_{tower}. Figure 1-left shows the p/E_{tower} spectrum for the electron candidates in which it is possible to see a well defined electron peak. The residual hadronic background is shown as a solid line in the spectrum. After hadronic background subtraction the electron peak is not centered at 1 due to the energy leakage to neighboring towers. The amount of leakage depends on the distance to the center of the tower hit by the electron and it is well descibed by GEANT simulations of the detector response.

The shower max detector plays an important role in the electron identification procedure. In general, hadronic showers are not well developed compared to electromagnetic showers in the shower max region of the EMC. The resulting differences are used to enhance the electron discrimination power. The procedure used in this analysis was to set high thresholds in the shower max shower reconstruction. Electrons will have showers reconstructed well with these cuts while hadrons will have very low efficiency shower reconstruction. We also compare the distance of the extrapolated particle to the reconstructed shower. Because of the poorly developed showers in the case of hadrons, this distance will have a much wider distribution, as seen in Figure 1-right. The overall electron identification efficiency was obtained by embedding simulated electrons into real events and was found to be $\sim 50\%$ and p_T independent for electrons with $p_T > 2$ GeV/c.

The electrons measured originate from various different sources. We classify two categories: (i) the physics signal, composed from semileptonic heavy quark decays and

Drell-Yan processes and (ii) the background sources. The background electrons are mainly from secondary electrons (photon conversions and Dalitz decays of light vector mesons) and hadrons misidentified as electrons. This background should be removed from the spectra in order to address the physics signal.

Most of photon conversion and π^0 Dalitz decays can be removed by calculating the invariant mass spectrum of di-electrons. Figure 2-left shows the m^2 spectrum for opposite and same charge electron pairs. A cut of $m^2 < 0.02$ $(\mathrm{GeV/c^2})^2$ removes most of the photon conversion and Dalitz decay electrons. The remaining background, mainly composed of η, ω, ϕ and ρ decays, was estimated from Pythia [6] and HIJING [7] simulations and it is on the level of a few percent of the total background. Figure 2-right shows the ratio between the physics signal to background electrons. The overall signal to background ratio improves substantially at high-p_T.

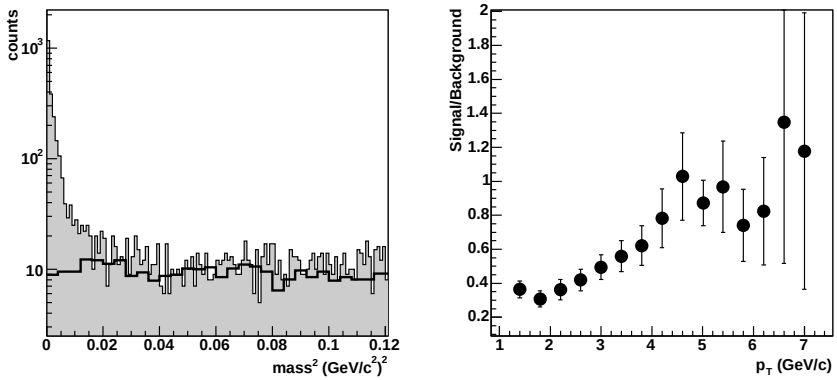

Figure 2. Left: $mass^2$ spectra for e^+e^- pairs (histogram) and same charge sign pair (line). Right: Signal to background ratio for electron as a function of electron p_T.

The hadron contamination was estimated by selecting hadrons using TPC dE/dx and computing how many of them are identified as electrons in the EMC. Residual hadronic contamination is on the order of 3% for $p_T = 2$ GeV/c and 8% for $p_T = 6$ GeV/c. By combining the TPC and EMC it is possible to achieve an e/h discrimination power on the order of 10^5 while maintaining an electron identification efficiency around 50%.

Figure 3-left shows the primary electron spectra for d+Au and p+p collisions at $\sqrt{s_{NN}} = 200$ GeV. The error bars are statistical errors and the boxes depict the systematic uncertainties.

The lines in the Figure 3-left show the electron spectra prediction for p+p collisions from Pythia simulations. The thick solid line is the total electron yield prediction while the thin solid and dashed lines are predictions for electrons from D and B mesons decays respectively. The dash-dotted line is the contribution to the electron spectrum for B mesons decaying into D mesons before decaying to electrons and the contribution to the total yield is negligible. The dotted line is the contribution from Drell-Yan to the electron yield. The Pythia parameters used in the current simulations are: $\langle K_T \rangle = 2$ GeV/c, $m_C = 1.7$ GeV/c^2, $K = 2.2$, CTEQ5M1 and $PARP(67) = 4$. It is important

to notice that the Pythia simulation is not a fit to the data but just a representation of what may be the sources of electrons observed and the parameters used are still under investigation. We note, however, that electrons at moderate to high p_T ($p_T > 3.5$ GeV/c) have a significant to dominant contribution from B decays, being the first RHIC measurement sensitive to beauty cross section. Figure 3-right shows the ratio, R_{dAu}, of the d+Au and p+p spectra, normalized for the number of binary collisions, as a function of p_T. It is important to notice that the electron R_{dAu} at a given p_T arises from a wide heavy-flavor p_T range. The ratio is approximately consistent with unity for the entire momentum range suggesting that the electron production in d+Au collisions follow a simple binary scaling from p+p collisions. A small Cronin type enhancement can not be ruled out. The magnitude of the Cronin effect for heavy quark mesons is not significantly different from that of light quark hadrons [8].

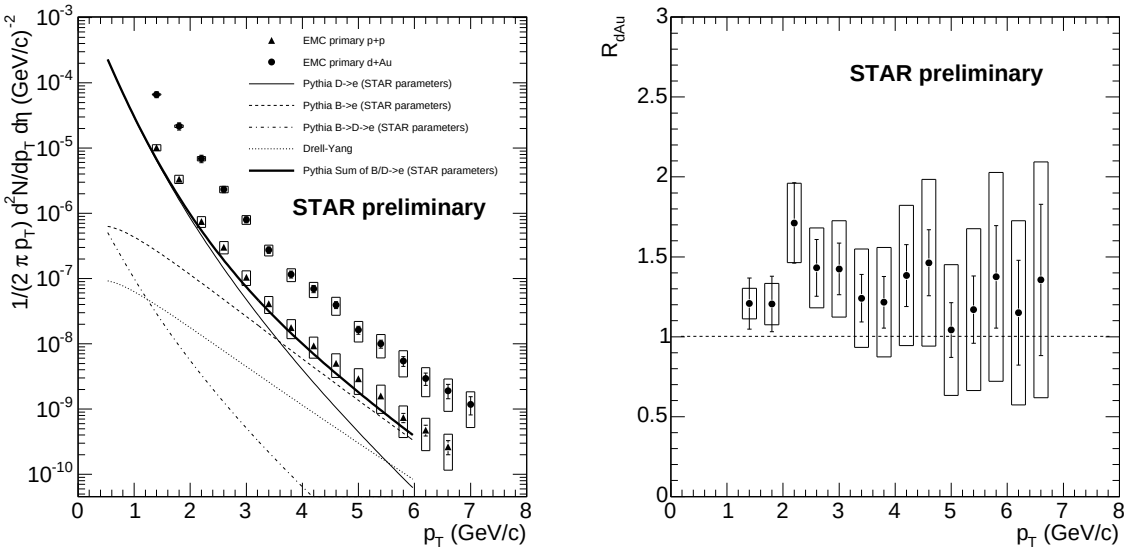

Figure 3. Left: Background subtracted electron spectra for d+Au (circles) and p+p (triangles) collisions. The error bars indicate the statistical errors and the boxes show the systematic uncertainties. The lines show Pythia simulations (see text for parameters). Right: R_{dAu} for electrons at $\sqrt{s_{NN}} = 200$ GeV. There is an overall normalization error of 17.4% on the unity that is not shown in the figure.

References

[1] B. Muller and X.N. Wang, Phys. Rev. Lett. 68, 2437 (1992).
[2] Yu. L. Dokshitzer and D.E. Kharzeeva, Phys. Lett. B 519 (2001) 199.
[3] C. Adler et al. STAR Collaboration, Phys. Rev. Lett. 89 (2002) 202301.
[4] M.C. Abreu et al. NA50 Collaboration, Phys. Lett. B 477 (2000) 28.
[5] K. H. Ackermann et al., Nucl. Instr. and Meth. A 499 (2003) 624, M. Anderson et at., Nucl. Instr. and Meth. A 499 (2003) 659 and M. Beddo et al. Nucl. Instr. and Meth. A 499 (2003) 725.
[6] T. Sjstrand, P. Edn, C. Friberg, L. Lnnblad, G. Miu, S. Mrenna and E. Norrbin, hep-ph/0010017 (2000).
[7] X. N. Wang and M. Giulassy, Phys. Rev. D 44, (1991) 3501.
[8] J. Adams et al. STAR Collaboration, Phys. Rev. Lett. 91 (2003) 072304.